

## Deformation and Ductile Cracking Behavior of X80 Grade Induction Bends

**Ryuji Muraoka, Nobuyuki Ishikawa and Shigeru Endo**

Materials and Processing Research Center  
NKK Corporation  
Fukuyama, Japan

**Masaki Yoshikawa**  
Engineering Research Center  
NKK Corporation  
Kawasaki, Japan

**Nobuhisa Suzuki**

Research and Development Division  
NKK Corporation  
Tokyo, Japan

**Joe Kondo**

Fukuyama Works  
NKK Corporation  
Fukuyama, Japan

**Masaaki Takagishi**

Dept. of Manufacturing Technology  
Dai-ichi High Frequency Co. Ltd.,  
Kawasaki, Japan

### ABSTRACT

Permanent ground movement is expected in seismic areas and in permafrost regions, and pipelines buried in those areas need to be designed to have sufficient deformability. Especially, bends need to have superior deformability, because it was pointed out in the recent earthquake event that deformation tends to concentrate in the connection region of pipelines. Severe deformation can lead to a fracture of the pipe wall and this may cause explosion of the pipeline or leakage of the gas, which need to be prevented in the areas with high population density. In spite of the importance of deformability for pipe bends, there are only a few reports on this issue. Furthermore, those investigations are limited for up to X65 grade induction pipe bends.

In this study, two types of API X80 grade induction pipe bends, 610mmOD x 11.0mmWT and 610mmOD x 16.6mmWT, bending radius of three times the pipe diameter and bending angle of 90 degree for both, were manufactured using longitudinally submerged arc welded pipes as mother pipes. And large scale bending test using X80 grade pipe bend was conducted by applying closing displacement on the tangents under the internal pressure of 12MPa by water. Bending load was continuously applied up to the maximum load point, and then prescribed displacement was applied until twice the maximum load point. Local deformation was shown in the middle of the bend portion, however, no cracking was observed. Furthermore, EF analysis of bending test was performed for precise estimation of stress/strain response of pipe bend, and analytical results were compared with experimental data. These bending tests proved that large deformability could be expected on the X80 grade pipe bends even under the high internal pressure.

In order to investigate ductile cracking behavior of the X80

grade induction pipe bend, notched round bar tensile tests were also conducted, and the criterion for ductile cracking was compared with X65 grade bend material. Relation between equivalent plastic strain and stress triaxiality at a ductile crack initiation point was determined by FE analysis, and this analysis proved that X80 grade bend material has enough resistance to ductile cracking compared to X65 grade bend. This result also corresponds to the results of the bend test, which is showing enough deformability of the X80 grade induction bends.

### INTRODUCTION

In the seismic areas like Japan, liquefaction or fault induced permanent ground displacement can cause severe damage to buried pipelines in a large earthquake. Also, in permafrost regions, a similar event is expected to occur by a large movement of ice ground. Large deformation of the pipeline can lead to cracking of the pipe body at the buckled region, resulting in a leakage or explosion of gases. Therefore, the buried pipelines in those areas need to be designed to have sufficient deformability and resistance to cracking. Especially, elbows and bends, the connection points of pipeline system, are required to show superior deformability, because deformation is concentrated to those parts for its lower stiffness compared to other straight part of the pipeline.

On the other hand, recent needs for a total cost reduction in fabrication and operation of pipeline system requires higher strength bends, as well as straight pipelines, because it enables to save material cost by reducing wall thickness. And significant cost reduction can be achieved by increasing service pressure in operation, and increasing design pressure is expected for higher grade linepipes. Many attempts have been made for developing

high strength induction bend pipes[1-4]. However, only a few investigations were reported for API X80 grade bend pipes[5,6], and further development is expected in order to fulfill the recent needs. Especially, deformation behavior of higher grade bend pipe has not yet been explored. There are only a few reports on large scale bending test of API X65 grade bend pipes or lower[7,8]. Two types of in-plain deformation mode, opening mode and closing mode, are considered for buried bend pipes. Based on the analytical study for X65 grade induction bend, it was pointed out that buckling is expected to occur at the transition region between the bend portion and the tangent under the opening mode deformation, while strain is concentrated in the center of the bend portion under the closing mode[9]. However, no large-scale bending test has been reported for X80 grade bend pipes.

Furthermore, cracking behavior after large deformation of higher grade pipe materials is of great interest, because preventing leakage or explosion of gases is key issue for the safety of gas pipeline system in the areas with high population density. Ductile fracture is accelerated by plastic strain and stress triaxiality[10], and the buckled region of the deformed pipe is a major initiation site for ductile cracking because of its geometrical discontinuity. Criterion for ductile cracking can be explained by the relation between equivalent plastic strain and stress triaxiality, and small scale test using notched round bar specimen is proposed for evaluating the resistance to ductile crack initiation[11,12].

In this study, API X80 grade induction bend pipes were manufactured and the closing mode bending test under the inner pressure was carried out, as a first step for investigating deformability of X80 grade bend pipes. Ductile fracture behavior of X80 bend pipe was also investigated by round bar tensile test.

## PRODUCTION AND PROPERTIES OF X80 GRADE INDUCTION BENDS

### Mother Pipe for Induction Bend

Longitudinally submerged arc welded pipes were used as mother pipes for the API X80 grade induction bend. The chemical composition for the mother pipe is shown in Table 1. Mo, Nb and other alloying elements were added to obtain enough strength, while C content and Ceq or Pcm values were restricted to lower values. The steel plates for mother pipes were produced applying

Table 1 Chemical compositions of the mother pipe(wt.%).

C	Si	Mn	Mo	Nb	others	Ceq	Pcm
0.06	0.24	1.82	0.17	0.04	Cu, Ni, V, Ti	0.44	0.19

Table 2 Mechanical properties of the mother pipe.

O.D. (mm)	W.T. (mm)	YS (MPa)	TS (MPa)	EI (%)	YR (%)
610	11.0	725	813	22	89
610	16.6	606	751	33	81

\*API full thickness specimen

controlled rolling followed by subsequent accelerated cooling process. Two sizes of mother pipes, those have different wall thickness of 11.0mm and 16.6mm, but same outer diameter of 610mm, were manufactured by UOE process. Mechanical properties of the mother pipes are shown in Table 2. Both pipes have enough strength as API-X80 grade and superior toughness, as well.

### Manufacturing Process of X80 Grade Induction Bend

There are mainly three types of manufacturing process for high strength induction bend pipes depending on heat treatment and the portion where heat treatment is applied[4]. The tempering free process, which quenching is applied only on the bend portion then tempering process is not applied, is an economical process, and can be applied up to API X65 grade. However, in order to balance strength and toughness for X80 grade bend pipe, it was reported that tempering can not be neglected, and full length quenching and tempering process, which both bend portion and tangent are quenched and tempered, was recommended for 20mm thick X80 grade bend pipe[9]. In spite of this suggestion for the manufacturing process of X80 grade induction bend, the partial quenching and tempering process, which quenching is only applied on the bend portion then all portion including tangents are tempered, was applied in this study. Since enough toughness of tangent can be obtained without quenching and only applying tempering for the thinner wall thick bend pipe using the mother pipe as mentioned in the previous section.

The schematic illustration of the X80 induction bend in this study is shown in Fig. 1. The bending radius was three times of the outer diameter of the mother pipe (3DR) and the bending angle was 90 degree. Induction heating subsequently followed by quenching with water cooling was applied on the bend portion, then all portion including tangents was tempered by furnace. Quenching and tempering temperature for both bend pipes were optimized so that enough strength and toughness for bend portion and tangent can be achieved.

### Mechanical Properties of X80 Grade Induction Bend

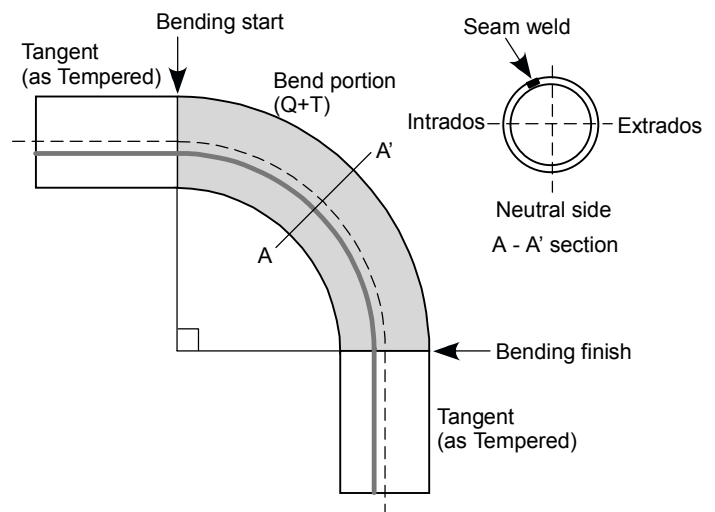


Fig. 1 Schematic illustration of the X80 grade bend pipe.

Table 3 Mechanical properties of X80 grade induction bend pipes.

Pipe Size		Position	Tensile properties			Charpy Impact test		DWTT
OD (mm)	WT (mm)		YS (MPa)	TS (MPa)	YR (%)	vE-80 (J)	vTs (deg. C)	SA at -20C (%)
610	11.0	Intrados	592	748	79	140	-84	100
		Extrados	566	740	76	117	-87	100
610	16.6	Intrados	555	716	78	148	-104	100
		Extrados	587	760	77	153	-77	100

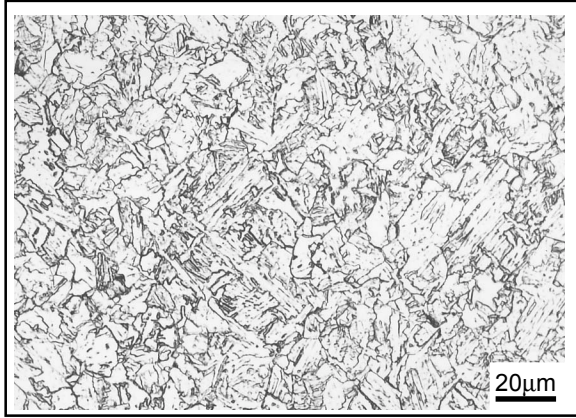


Fig.2 Microstructure of X80 grade bend pipe.

Close material examination was carried out on the various portions of the bend pipe including extrados and intrados of the bend portion. Mechanical properties of X80 grade induction bend pipes are shown in Table 3. Tensile test were performed by using API standard full-thickness strip specimens in the transverse direction, which is obtained by flattening of the pipe body. Charpy impact specimens were taken in the transverse direction in the mid thickness. Full-thickness DWTT specimens were taken in the transverse direction.

Both types of bend pipes showed enough strength in all position of the bend portion as API-X80 grade. Sufficient low temperature toughness was obtained for both portions. Fig.2 shows microstructure of X80 grade bend pipe in the mid-thickness region. Fine bainitic microstructure was obtained in the bend portion. The microstructure of the steel plate that was controlled rolled and accelerated cooled was maintained in the tangent, where only tempering was conducted.

## DEFORMATION OF PRESSURIZED X80 BENDS

### Procedure of Full-scale Bending Test

In order to investigate deformability of X80 grade bend pipe, full-scale bending test were conducted under the closing mode in-plane deformation, which buckling occurs in the bend portion. Test was conducted at ambient temperature of about 15°C under internal pressure by water. Manufactured 11.0 mm thick X80 grade induction bend was used for the full-scale test. Fig.3 shows schematic illustration of the bending test apparatus. Both end of

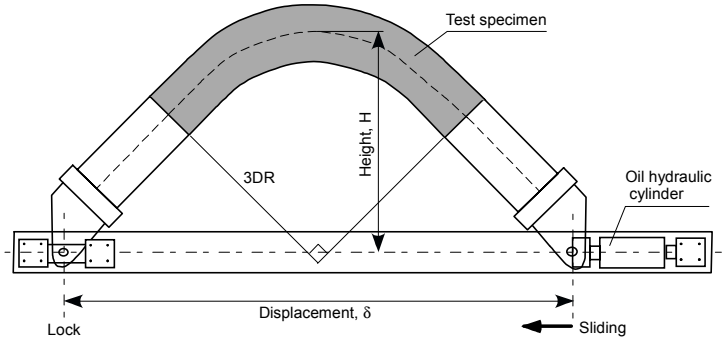


Fig.3 Bending test apparatus.

the bend pipe were connected to the loading arm, and closing mode displacement was applied by a hydraulic jack under the loading speed of about 0.2mm/s. Internal pressure of 12MPa, which is equivalent to 0.72 times specific minimum yield stress by hoop stress of bend portion, had been kept during the test.

In order to measure strain distribution in the bend portion during the bending test, bi-axial strain gauges were mounted on the outer surface of the bend portion around the central region by the intervals of 45 degree in the circumferential direction. Bending angle was measured by the angle meter, which is attached at the tangent portion of the specimen.

In this test, closing mode displacement was applied up to twice of the displacement at maximum load point ( $2\delta_{pmax}$ ). Bending load, displacement, bending angle and strain were monitored and recorded continuously throughout the test.

### Results of Bending Test

Fig.4 shows the relationship between applied load (P) and displacement ( $\delta$ ) in the full-scale bending test. Applied load increased linearly with displacement in elastic region at the first stage of the bending test. Deformation mode of test specimen changed from elastic region to plastic region. The maximum load and the displacement at maximum load point were  $993 \times 10^3$  kN and 540mm, respectively. After the maximum load, buckling started to occur in the center region of the bend portion, and then load decreased gradually with increasing displacement. Loading was terminated at displacement twice the displacement at maximum load.

Fig.5 shows overviews of test specimen before bending, at

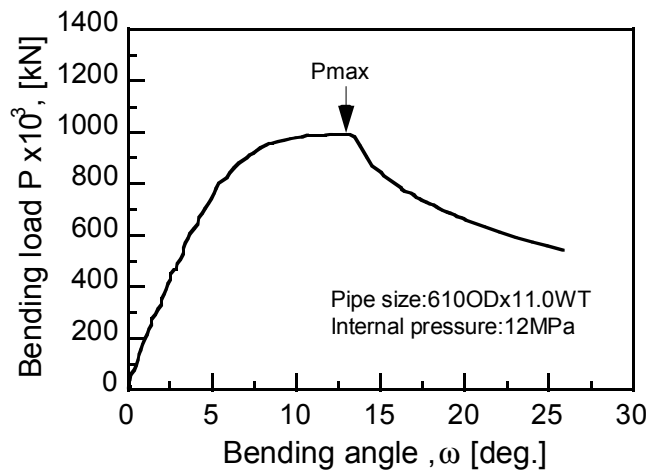


Fig.4 Bending load versus bending angle curve in the full-scale bending test.

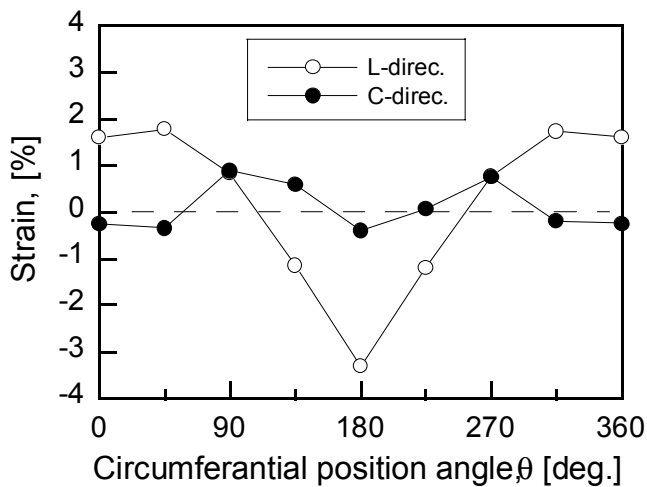


Fig.6 Strain distribution in center section at maximum load.



(a) Before bending



(b) Maximum load ( $\delta = \delta_{pmax}$ )



(c)  $\delta = 2\delta_{pmax}$

Fig.5 Overviews of the test specimen during bending.

Table 4 Full-scale bending test results of X80 grade bend pipe.

Pipe Size OD (mm)	WT (mm)	Maximum Load $\times 10^3$ (kN)	Maximum Moment (Nm)	$\omega_{pmax}$ (deg.)	Max. Strain at $\omega_{pmax}$	
					L-direc. (%)	C-direc. (%)
610	11.0	993	2597	13.1	-3.3	+1.8

the maximum load and at  $\delta = 2\delta_{pmax}$ . Buckling toward inside of the bend portion was observed at the central section in intrados side after maximum load. At the displacement of  $\delta = 2\delta_{pmax}$ , large wrinkle shape by buckling of the intrados was seen, however, no cracking was observed even after reverse displacement while unloading. Fig.6 shows the measured strain distribution in the central section at maximum load. In Fig.6, extrados and intrados are located at  $\theta = 0$  degree and 180 degree, respectively. The intrados, where  $\theta = 180$  degree, showed large compressive strain of 3.3% in the longitudinal direction, and maximum tensile strain was 1.8% at  $\theta = 45$  and 315 degree. On the other hand, in the longitudinal direction, the position at  $\theta = 90$  and 270 degree



showed higher tensile strain because of flattening of the pipe section.

Results of bending test were summarized in Table 4. The bending angle at maximum load,  $\omega_{pmax}$ , was 13.1 degree, where bending angle is defined as the difference in the angle of two tangents. Experimental investigation on deformability of pressurized pipes was quite limited as mentioned before. However, it was reported that X65 grade linepipe (straight pipe) showed  $\omega_{pmax}$  of around 10 degree in pressurized bending test, which hoop stress corresponds to 0.4 times SMYS[12]. In this study, the X80 grade bend pipe was tested under the inner pressure of 0.72 times SMYS by hoop stress, but bending angle to maximum loading was higher than that of X65 linepipe test. Although, further investigations are necessary to insure the reliability against large deformation, it is considered that X80 grade bend pipe has enough capacity of stable deformation even under high internal pressure.

### Numerical Analysis

FE analysis was carried out for the purpose of evaluating stress and strain states of specimen. FE program code of ADINA Version 6.3 was used. For elasto-plastic analysis, the Von Mises's material model was employed. Fig.7 shows the 4-Node shell element mesh for pipe bend.

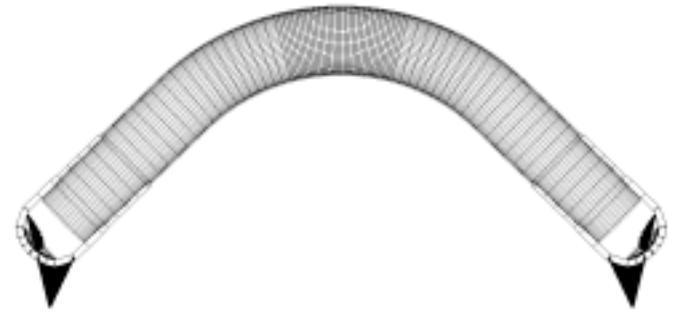


Fig.7 4-Node shell element mesh for pipe bend.

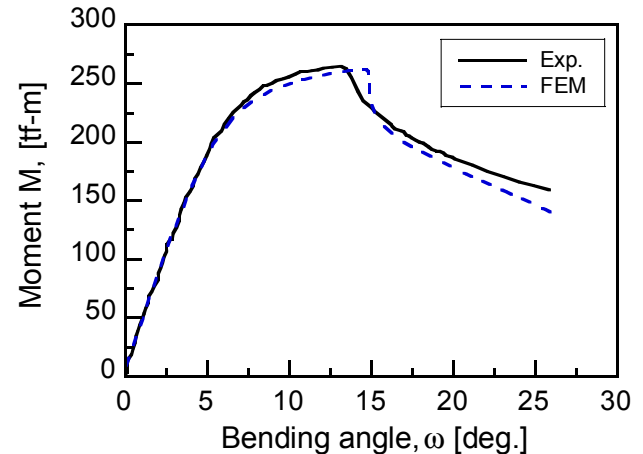


Fig.8 Comparison of bending moment versus bending angle curve between experiment and numerical analysis.

### Numerical Analysis Results

Analytical result was macroscopically compared with experimental result. Fig.8 shows the relationship between bending moment  $M$  at the central section of the specimen and the bending angle  $\omega$  by experiment and numerical analysis. The calculated bending angle at maximum moment point was approximately 14.5 degree and it is observed that the experimental value and the calculated value corresponded well.

Comparison of analytical result and experimental result was microscopically inspected. Fig.9 and Fig.10 show the comparison of circumferential strain distribution in the central section of the specimen between experimental strain and calculated strain at applied displacement  $\delta$  of 100mm and 500mm, respectively. Large compressive strain in the longitudinal direction was shown at  $\theta = 135$  and 225 degree and maximum tensile strain in the circumferential direction was shown at  $\theta = 90$  and 315 degree in elastic deformation region of  $\delta=100$ mm. In the plastic region of  $\delta=500$ mm, maximum compression strain was shown in the longitudinal direction at the intrados side and maximum tensile strain was shown in the longitudinal direction near the extrados side. The experimental and analytical results are corresponded well.

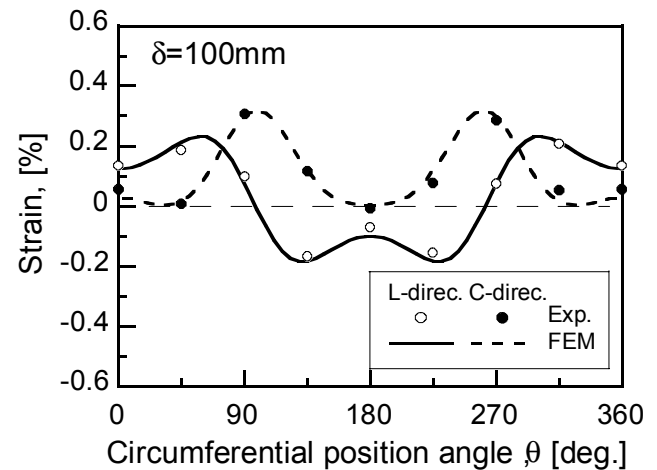


Fig.9 Comparison of circumferential strain distribution at  $\delta=100$ mm between experiment and numerical analysis.

Fig.11 and Fig.12 show the comparison of longitudinal strain distribution in the central section of the specimen between experimental and analytical results at applied displacement  $\delta$  of 100mm and 500mm, respectively. Longitudinal position angle  $\theta'$  was defined as the degree from the center of bend portion. In the elastic region, longitudinal and circumferential strains were constant at each longitudinal angle. Tensile strains were shown at the extrados and compressive strains were shown at the intrados. In the plastic region, longitudinal strains at the extrados were approximately 1.2% in constant at each longitudinal angle. At the intrados, maximum compressive strain was shown 2.2% at

$\theta'=0$ . The experimental and analytical results are corresponded well.

Fig.13 shows the relationship between maximum strain and bending angle by experiment and analysis. Maximum strain was shown in the longitudinal direction at intrados side of central section. The rapid rise in maximum strain was shown at  $\omega=13$  to

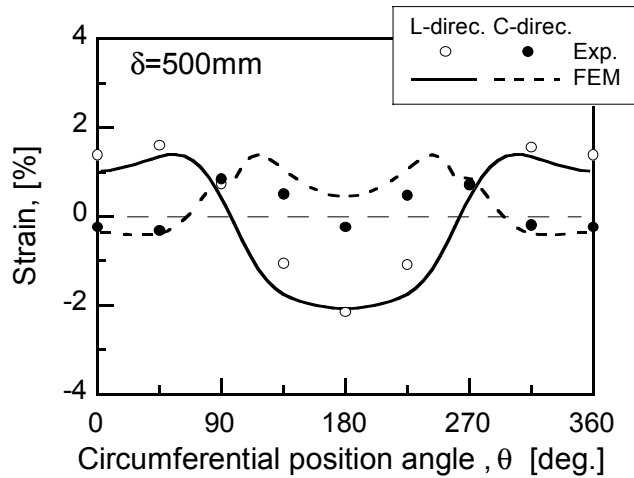
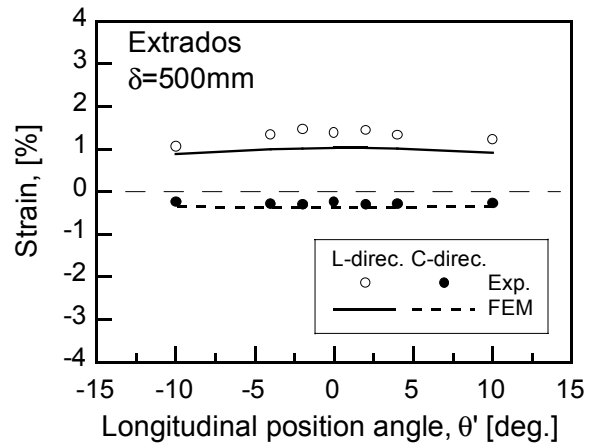
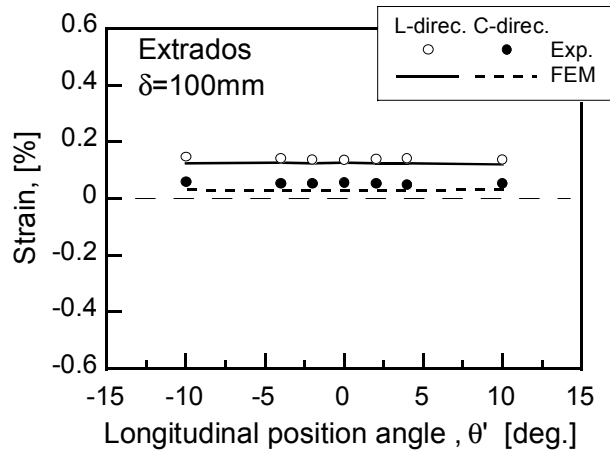


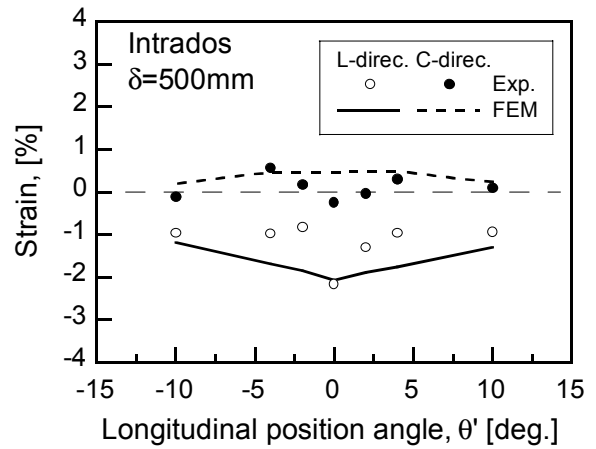
Fig.10 Comparison of circumferential strain distribution at  $\delta=500\text{mm}$  between experiment and numerical analysis.



(a) Extrados side

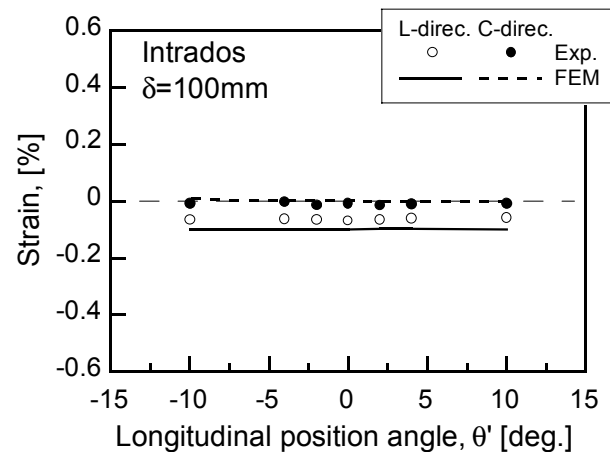


(a) Extrados side



(b) Intrados side

Fig.12 Comparison of longitudinal strain distribution at  $\delta = 500\text{mm}$  between experiment and numerical analysis.



(b) Intrados side

Fig.11 Comparison of longitudinal strain distribution at  $\delta = 100\text{mm}$  between experiment and numerical analysis.

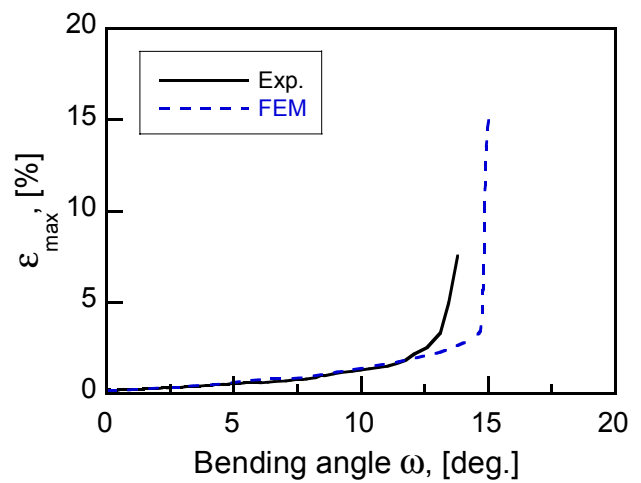


Fig.13 Comparison of maximum strain versus bending angle curve between experiment and numerical analysis.

15 in the experimental and analytical results, and both results are corresponded well.

Accordingly, it was considered that deformation behavior of X80 grade bend pipe was expected well under other conditions of bending tests.

## DUCTILE CRACKING BEHAVIOR

### Notch Round Bar Tensile Test

As pointed out by Toyoda et. al., ductile cracking can occur in the buckled region of bent pipe in reverse loading. Ductile crack initiation behavior is affected by stress triaxiality, ratio of hydrostatic stress to equivalent stress, and equivalent plastic strain, and critical conditions can be evaluated by combined investigation of small scale tensile test and FE analysis.

Ductile cracking property of X80 grade induction bend material was determined using notched round tensile test. Fig. 14 shows configuration of notched round bar specimen. Notch root radius was changed from 0.5mm to 2.0mm in order to obtain different stress condition around notch region. In order to compare the ductile cracking behavior of X80 bend with ordinal bend material, X65 grade induction bend produced by the tempering free process was also used for the test.

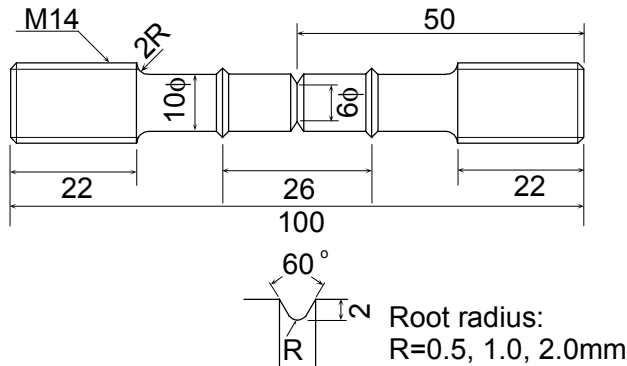


Fig.14 Configuration of notched round bar specimen.

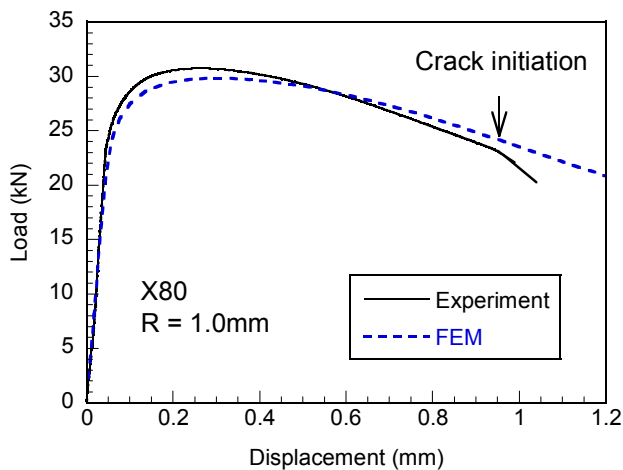


Fig.15 Load-displacement curves.

Fig. 15 shows the load-displacement curve of X80 bend by the specimen with root radius of 1mm. Experimental curve has a discontinuous point caused by ductile cracking in the specimen center. Ductile crack initiation point was determined by metallurgical observation of the notch section using several specimens with same root radius but loading were stopped by different displacement. Ductile cracking occurs by coalescence of voids, as shown in Fig. 16. Void growth is strongly affected by triaxial stress state, and the stress triaxiality dependence of ductile cracking behavior can be determined by using notched specimens with different notch root radius.

### Criterion for Ductile Cracking

Critical conditions for ductile crack initiation were evaluated by FE analysis. Axisymmetric second order elements were used in order to model notched round bar specimen, as shown in Fig. 17. FE program use for the analysis was ABAQUS ver. 5.8. Mises plasticity and isotropic hardening model for material property were used in the non-linear stress/strain analysis. The calculated load-displacement curve for X80 induction bend is compared with experimental curve as indicated in Fig. 15, and good agreement of those curves can be seen up to ductile crack initiation point. Ductile crack initiated in the specimen center for the specimen with  $R=1.0\text{mm}$  and  $2.0\text{mm}$ , while cracking was observed in the notch tip (from surface) for the  $R=0.5\text{mm}$  specimen, and equivalent plastic strain and stress triaxiality in the critical region where ductile cracking occurs were calculated by FE analysis. Equivalent plastic strain to ductile crack initiation for X80 and X65 induction bend was plotted in Fig. 18 as a function of stress triaxiality. Ductile cracking behavior of many other structural



Fig.16 Ductile cracking of X80 in the center of the specimen with  $R=1.0\text{mm}$ .

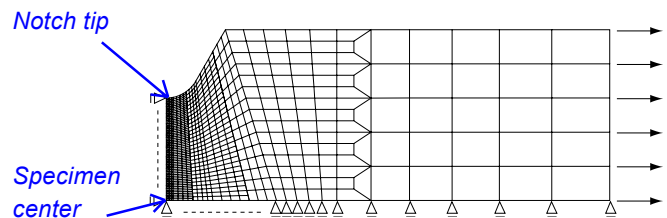


Fig.17 Mesh division for the notched specimen with  $R=1.0\text{mm}$ .

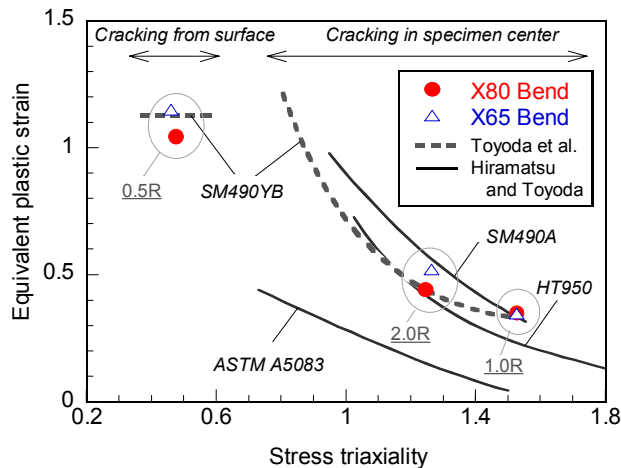


Fig.18 Relation between equivalent plastic strain and stress triaxiality at ductile crack initiation.

steels was investigated and criterion for ductile crack initiation was compared with the results of X80 and X65 grade pipe bends, as indicated in Fig. 18. Equivalent plastic strain to ductile cracking decreases with increasing stress triaxiality for all steels, because void growth is accelerated under high triaxial stress state. X80 induction bend gave almost the same critical condition as X65 grade induction bend, and also similar to many other structural steels, excepting ASTM A5083 steel. These results of criterion for ductile cracking show that X80 grade induction bend has the same resistance property against ductile fracture as ordinary X65 bend.

## CONCLUSION

In order to evaluate deformation under internal pressure and ductile cracking behavior of X80 grade induction bends, two types of API X80 grade induction bend pipes with 610mmOD x 11.0mmWT and 610mmOD x 16.6mmWT were manufactured by partial Q-T process using longitudinally submerged arc welded pipes as mother pipes. The closing mode bending test of X80 grade bend pipe under the internal pressure of 12MPa by water was carried out and numerical analysis was performed. Furthermore, notched round bar tensile tests were also conducted, and the criterion for ductile cracking were compared with X65 grade bend material. Relation between equivalent plastic strain and stress triaxiality at ductile crack initiation point was determined by FE analysis. The results were summarized as follows.

- (1) Two types of X80 grade induction bend pipes manufactured showed sufficient properties as API-X80 grade.
- (2) This bending test proved that enough deformability could be assured for the X80 grade bend pipes even under the high internal pressure.
- (3) Both experimental result and analytical result were corresponded well. It was considered that deformation behavior of X80 grade bend pipe was expected well under other conditions

of bending tests.

(4) The analysis proved that X80 grade bend material has enough resistance to ductile cracking compared to X65 grade bend. This result also corresponds to the results of the bend test, which is showing enough resistance to leakage for the X80 grade induction bends.

## REFERENCES

1. Viatour, P., Bosteels, H. and Messin, P., "Induction Bending of API Grade Line Pipe," Pipe Line Industry, May (1983), pp. 33-40.
2. Hirano, O. and Akao, K., "High Strength Arctic-Grade UOE-Pipe for Induction Bending," Nippon Kokan Technical Report Overseas, 46 (1986), pp. 101-105.
3. Hashimoto, T., Komizo, Y., Sawamura, T., Nakada, H. and Nakatsuka, Y., "High Strength Hot-Bent Pipe for Arctic Use," Transaction ISIJ, 26 (1986), pp. 418-424.
4. Kondo, J., Nagae, M., Hirano, O. and Takagishi, M., "The State of the Art of Induction Bent Pipe," Proceedings of the 4th International Offshore and Polar Engineering Conference, Vol II (1994), pp. 164-171.
5. Graf, M. K., Hillenbrand, H. G. and Niederhoff, K. A., "Production of Large Diameter Linepipe and Bends for the World First Long-Range Pipeline in Grade X80 (GRS 550)," Proceedings of 8th Symposium on Line Pipe Research, (1993), pp. 5.1-5.14.
6. Ishikawa, N., Endo, S., Kondo, J. and Takagishi, M., "Development of X80 Grade Induction Bend Pipe," Proceedings of OMAE'02, OMAE2002-28182, (2002).
7. Katoh, A., Ono, Y., Yoshikawa, M. and Suzuki, N., "A Study on the Strength of Steel Pipe Bend Subjected to Large Displacement," PVP Vol. 371, High Pressure Technology, (1998), pp. 101-106.
8. Yoshinari, H., Oguchi, N., Uchida, T., Tatematsu, H., Katoh, A. and Yoshikawa, M., "Influence of Stress Triaxiality on Crack Initiation in Steel Pipe Bend Subjected to Large deformation," Engineering Fracture Mechanics, to be published.
9. Yatabe, H., Fukuda, N., Masuda, T. and Toyoda, M., "," Proceedings of the 20th International Offshore and Polar Engineering Conference, OMAE2002-28209 (2002).
10. McClintock, F. A., "A Criterion for Ductile Fracture by Growth of Holes," J. Appl. Mech., 35 (1968), pp. 363-371.
11. Toyoda, M., Ohata, M. and Yokota, M., "Criterion for Ductile Cracking for the Evaluation of Steel Structure under Large Scale Cyclic Loading," Proceedings of OMAE'01, OMAE2001/MAT-3103, (2001).
12. Hiramatsu, H. and Toyoda, M., "Ductile Crack Initiation Behavior of Various Structural Materials with Reference to Initiation /Growth of Voids," J. Soc. Naval Architects of Japan, 190 (2001), pp. 591-598.
13. Effect if a Straub Hardening Exponent on Inelastic Local Buckling Strain and Mechanical Properties of Line Pipes," Proceedings of OMAE'01, OMAE2001/MAT-3104, (2001).